PROCEEDINGS, 43rd Workshop on Geothermal Reservoir Engineering
Stanford University, Stanford, California, February 12-14, 2018
SGP-TR-213

Bwengwa River, Zambia – Exploration of a Non-Volcanic African Geothermal System

Maxwell Wilmarth[1], Jill Haizlip[1], Nicholas Prina[1], and Peter Vivian-Neal[2]

[1]GEOLOGICA GEOTHERMAL GROUP, INC., 5 Third Street, Suite 420, San Francisco, CA 94103, USA

[2]Kalahari GeoEnergy Ltd, 40 Jesmondine (Corner Central St & Mwambula Rd), Lusaka, Zambia

mwilmarth@geologica.net

Keywords: exploration, Zambia, resource assessment

ABSTRACT

The Bwengwa River geothermal field is a moderate-temperature fault-based geothermal reservoir located along a northeast-trending northwest-dipping normal fault associated with prolific near-boiling hot springs and terrace deposits. Temperature gradient hole drilling has encountered a more than 100°C reservoir at the faulted contact with the Proterozoic basement. Fluid geochemistry and cation geothermometry are consistent between the well fluids and the hot springs and indicate a deeper reservoir of ~150°C. Magnetotellurics, gravity, 3D magnetic modeling, and structural mapping indicate subsidiary conjugate faults to the main fault zone. The conceptual model of the reservoir has been updated for use in exploration well targeting and for an initial resource capacity estimate. A probabilistic power density estimate of a discovered 150°C resource yields an expected power capacity of 2-93 MWe (P90-P10) with a most likely value of 15 MWe (P50). Further planned exploration may increase this capacity estimate and confidence level.

INTRODUCTION

Kalahari GeoEnergy Ltd (KGE) is exploring the Bwengwa River Geothermal Resource Area (BWGRA, Bwengwa) within the Kafue Trough in southwestern Zambia (Figure 1). This area includes the Bwanda, Gwisho, Malundu and Namulula hot springs, all located along the Southern Bounding Fault (SBF) of the Kafue Trough. In 2012 KGE engaged GEOLOGICA GEOTHERMAL GROUP, INC. (GEOLOGICA) to assist with exploration and resource assessment. To date the exploration of Bwengwa has included geological, geochemical, and geophysical surveys including resistivity, gravity, and ground magnetics, among others. Six temperature gradient holes (TGHs) have been drilled up to depths of 577 m. Several of these have flowed spontaneously which yielded water samples for analysis. KGE's goal is to initially develop a ~10 MWe power generation project with cascading direct uses.

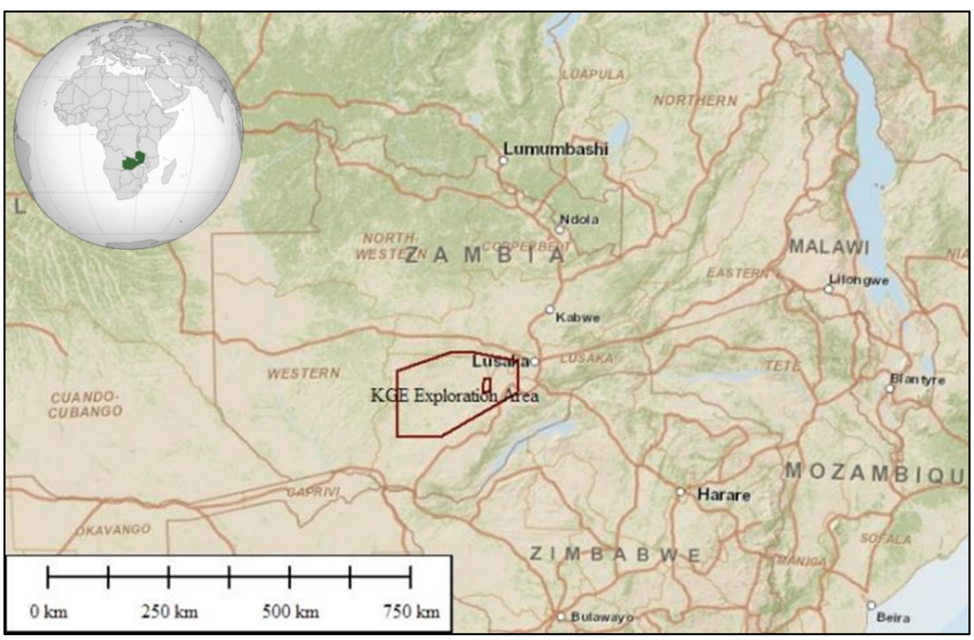

Figure 1. Location map of the KGE Exploration Area in Zambia.

GEOLOGY

Regional geologic setting

The BWGRA is located in the Kafue Trough, a NE-trending graben in the Southern Province of Zambia. The Kafue Trough is the southwest continuation of the larger NE-SW trending Luangwa and Luano Grabens, which are part of the southwestern branch of the East African Rift system (Figure 2).

The Kafue Trough is a graben that plunges to the southwest where it joins the Barotse Basin, an expansive Karoo basin with unconsolidated Kalahari sand cover. It is bounded to the south by Proterozoic crystalline rocks of the Choma-Kalomo block, which constitute the basement of the area. To the north, the Kafue Trough is similarly bounded by the Proterozoic rocks of the Kafue Hook Granite and Mwembeshi Gneiss Complex. To the east, the Kafue Trough is separated from the Luano Graben by metamorphic rocks of the Zambezi belt.

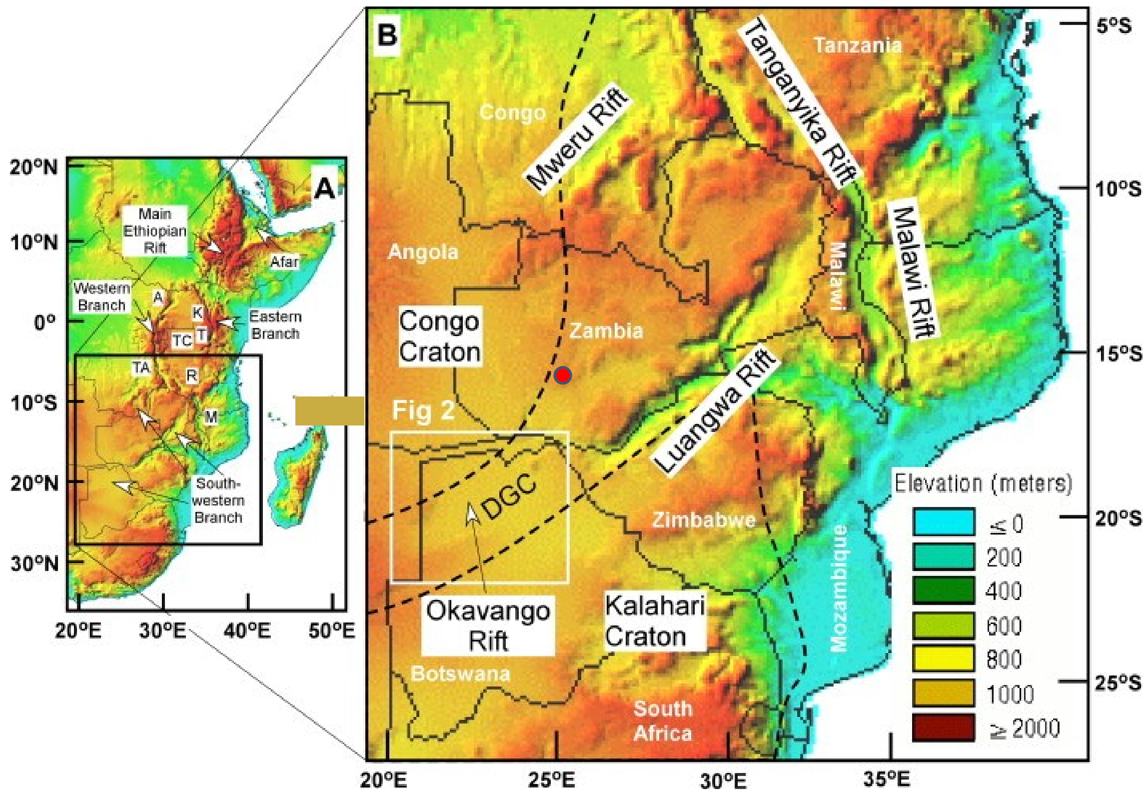

Figure 2. The East African Rift System (Bufford et al., 2012). The Luangwa Rift is part of the Southwestern Branch. Approximate project location indicated with red circle.

<u>Stratigraphy</u>

The subsurface geology in the Kafue Trough is largely obscured by alluvial sediments of the Kafue Plains, which overlie the Karoo, Katanga, and Basement Supergroups. There are few boreholes to ascertain the detailed stratigraphy and structure in the area. Most outcrops of Karoo and Katanga sedimentary rocks and the underlying crystalline basement are located on the margins of the basin.

The basement complex in the area consists of mid- and late Proterozoic metamorphic rocks (gneiss, quartzite, marble, and schist) and granitic rocks (granite, granodiorite), which intrude the older metamorphic rocks.

The crystalline Proterozoic complex is unconformably overlain by the Katanga Supergroup. The Katanga consists of marine sedimentary rocks and carbonates of Proterozoic to Ordovician age. The lower part of the almost exclusively sedimentary sequence is the economically important Mine Series Group, which hosts the bulk of the copper-cobalt mineralization in the Copperbelt. The Katanga Supergroup also includes minor schist units.

Overlying the Katanga and separated by an unconformity, is the Karoo Supergroup, a sedimentary succession of Carboniferous to Jurassic age. The Karoo Supergroup is subdivided into Lower Karoo and Upper Karoo Groups. The Lower Karoo consists of basal conglomeritic sandstones, referred to as the Dwyka unit south of the Zambezi, mudstone or argillaceous limestone, and minor coal beds (Harrison, 2012). The Upper Karoo consists of a lower unit of coarse-grained, feldspathic sandstone (called the Karoo grit) and basal conglomerate, which is succeeded by sandstone and mudstones, overlain by basalt (Harrison, 2012). Sandstone, which is the dominant lithology in the Upper

Karoo, forms most of the outcrops; they are usually coarse-grained and gritty close to the margin of the Karoo outcrop and become finer grained towards the center.

The larger part of the basin is filled with Quaternary-Tertiary sands of the Kalahari Group and alluvium of the Kafue Flats.

Structure

The primary regional structure is the NE/SW-trending Kafue Graben, which is about 65 km wide and about 145 km long. The graben is structurally bounded to the north and northwest by the Mwembeshi Dislocation Zone (MDZ), a wide zone of faulting and shearing extending from western Zambia northeast into Malawi. The southern and southeastern boundary of the Kafue Graben is similarly a zone of faulting, which trends northeast. The southern boundary fault (SBF) is a normal fault, which dips to the northwest, juxtaposing Karoo and Katanga rocks with basement and forming the contact that is the locus of the Lochinvar group of hot springs. The Karoo dips at shallow angles to the northwest and north towards the center of the basin of deposition. In the Lochinvar vicinity, the dips at surface between the SBF and the Upper Karoo vary from 3° to 27° (Harrison, 2012).

The NE-trending faults predominate in the region, probably following earlier lines of weakness in the basement related to the northeast Irumide Belt structural trends.

WNW-trending late Proterozoic faults and shear zones are prominent in the topography of Proterozoic outcrops but may have played only a minor role in the evolution of the Kafue Graben, where the dominant structural elements are northeast trending. However, the intersection of these two fault trends may be a controlling factor governing the locations of current hydrothermal activity.

Geology of the Bwengwa Geothermal Field

The Lochinvar hot springs are located on the southern boundary of Lochinvar National Park northwest of Monze Town. The springs extend along the SBF of the Kafue Graben for a distance of 6.6 km with high concentration of spring 'eyes' or zones of altered ground free of vegetation around Gwisho and Bwanda hot springs (Figure 3). They occur at the slope break on the fault itself.

According to Legg (1974), the SBF fault zone consists of a number of closely-spaced, sub-parallel faults, dipping steeply to the northwest, and with a total offset to the northwest between 1 and 1.5 km. The SBF segment along which these hot springs are aligned is believed to be the near-surface contact between the Katanga and Proterozoic rocks to the southeast and the Karoo Supergroup rocks (underlying the alluvium) to the northwest. This fault zone hosts re-crystallized quartz with calcite cement in some instances. Vugs are common in the fault breccia with quartz in-fills. In the southern part of the area near Mulundu and Namulula hot springs, there are spring deposits and alteration that indicate activity in the recent past that is now dormant.

The main rocks exposed at the surface (SE of fault) are quartzites and gneisses, which are well foliated, have a constant ESE strike, and generally dip toward the NNE. Rock exposures near the fault zone are fractured and traversed by narrow veins containing quartz (Legg, 1974). The quartzite near the Namulula hot spring is composed of quartz, amphiboles, epidote, and chlorite, all consistent with >350°C metamorphism rather than the current hydrothermal activity. The quartzite is highly jointed in parts with smooth joint surfaces, trending 290/70SW and occasionally in-filled with quartz. Proterozoic basement limestone is exposed at Drum Rock close to the SBF.

The Karoo rocks are represented by the whitish, feldspathic sandstone around Sebanzi Hill (SW of Gwisho Springs), which is bound by faulting. The sandstone is cut by crisscrossing quartz veins similar to those in the main fault breccia. Southeast of the SBF, the Katanga rocks consist of marble and pink quartzite in the central and southwestern areas while Proterozoic granitic gneiss comprises the northeastern area. The foliation in both the quartzite and granitic gneiss trends about 105/45NE. A geologic map of Lochinvar hot springs prepared by Legg (1974) is shown in Figure 4.

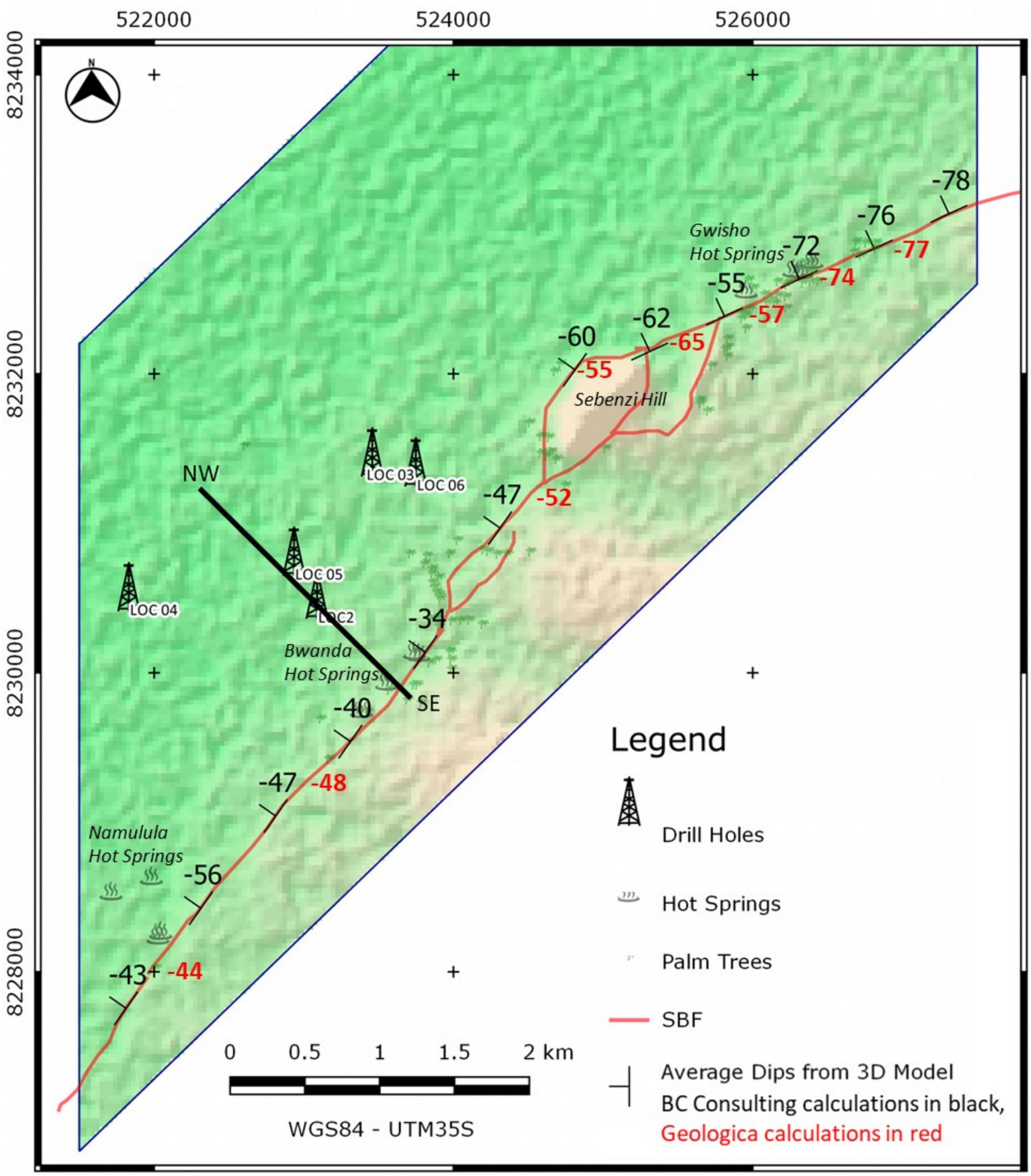

Figure 3. Map of Bwengwa Geothermal Field with cross section lines used in this report. Dip on the Southern Bounding Fault zone (SBF) based on 3D modeling of 2017 magnetic survey data. After BC Consulting (2017) with modeled dips checked by GEOLOGICA (in Red). Note well Loch-01 is located just off the northern extent of this map.

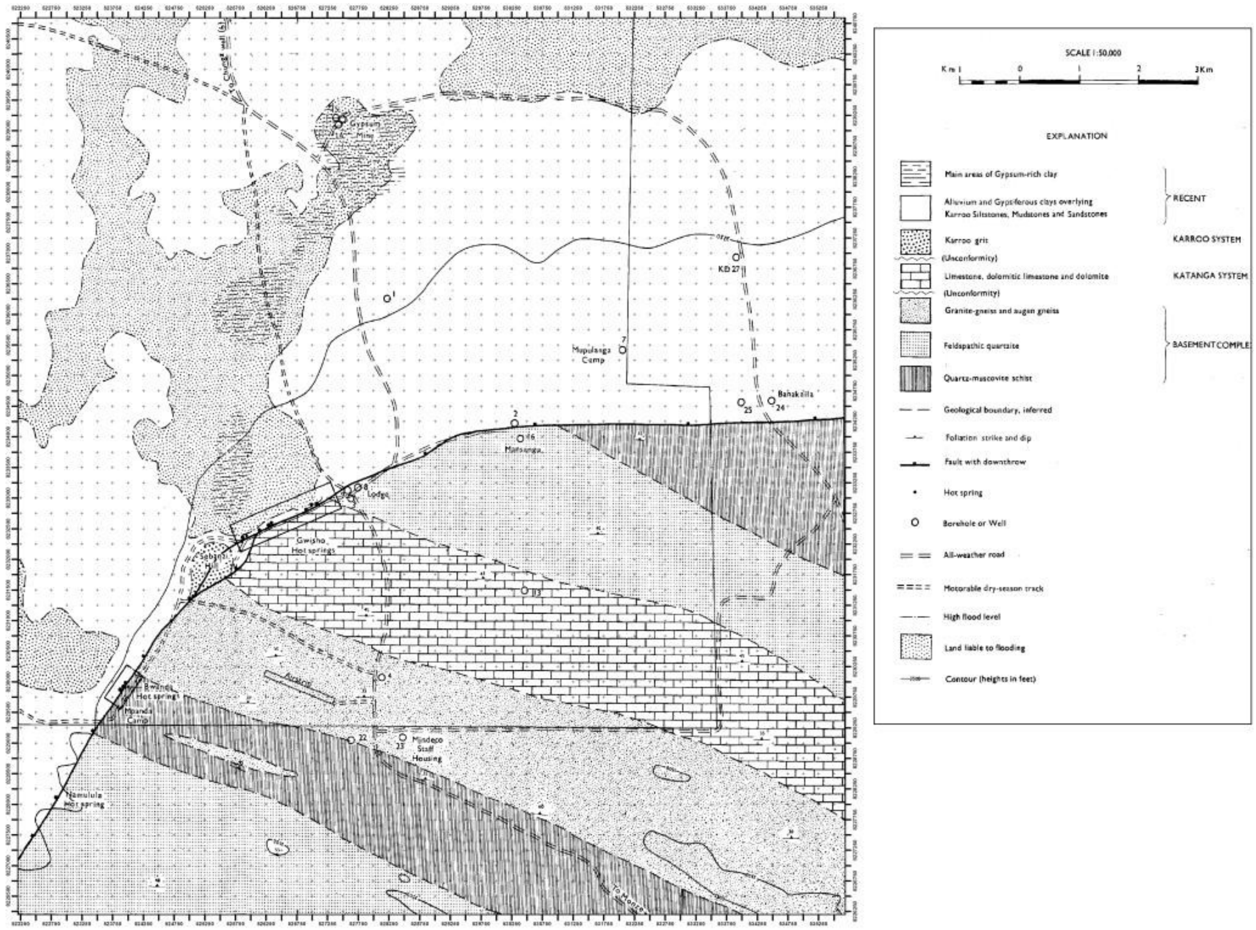

Figure 4. Geologic map of Lochinvar Hot Springs (Legg, 1974).

GEOCHEMISTRY

The Bwengwa geochemical database includes >60 geothermal water samples collected between 2010-2017 from the Bwengwa river geothermal area and four groundwater samples taken between 2013-2014 from nearby ground water sources. This includes water samples collected from the Bwanda and Gwisho hot springs, and TG holes Loch-02, Loch-03, Loch-04 and Loch-05 (Figure 3).

Water Type

Thermal waters from Bwengwa are all sodium (Na)-sulfate (SO_4)-chloride (Cl) type waters. This composition is within the range of non-magmatic geothermal systems which are typically lower in chloride and anions are dominated by SO_4 or bicarbonate (HCO_3). Elevated SO_4 may be related to the dissolution of gypsum known to be present in nearby shallow formations in the Bwengwa River area. The concentrations of major chemical constituents of near-boiling waters of Bwanda Hot Spring (~92-95°C) and wells Loch-02 (102-105°C) and Loch-05 (~100°C) are almost identical (within 10% relative percent difference). While the Gwisho hot spring have a similar composition, the concentrations are different and the fluid is slightly cooler (~75°C). Furthermore, the concentrations of all major solutes are higher in concentration (~30%). Based on the increase in concentration of all of the major chemical constituents (although to varying degrees) this difference between Gwisho and Bwanda is likely the result of evaporation rather than chemical or water/rock reaction, but could also be the result of mixing with cold groundwater high in dissolved solids (TDS).

Comparison of the relative major cation and anion chemistry of Bwanda, Gwisho, and the TG holes shows that each location hosts water of a similar composition with a few minor exceptions in cation chemistry (Figure 5). All samples have very similar relative concentrations of major anions (Figure 6). Although there is some variation in the minor chemical constituents (concentrations <1 mg/kg), the variation is likely not significant as the concentrations are so small. This suggests that waters from Bwanda, Gwisho, Loch-02, Loch-03, Loch-04, and Loch-05 have a common source; and the thermal waters from Bwanda, Loch-02 and Loch-05 have followed a similar pathway along the SBF such that the fluids have not been affected by different process. In contrast, the other thermal waters have been affected by other processes such as conductive cooling, evaporation, etc. (Figure 7).

Stable isotopes (oxygen-18 and deuterium) indicate waters from Loch-02 and Bwanda are related, however, the Loch-02 samples appear to be shifted towards heavier oxygen. This may be attributable to greater water-rock interaction in Loch-02 fluids due to either proximity to higher temperature fluid sources, or to greater dilution by meteoric water in the Bwanda springs.

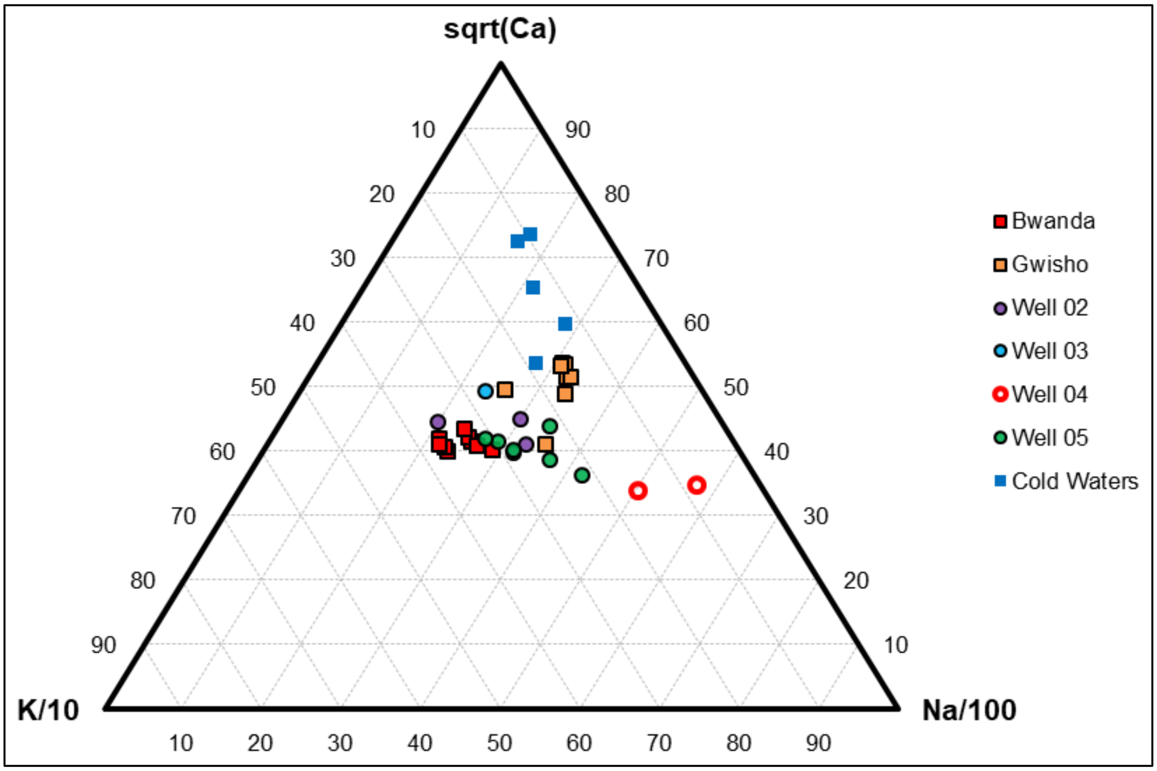

Figure 5. A trilinear diagram relating the relative concentration of major cations for samples from Bwengwa.

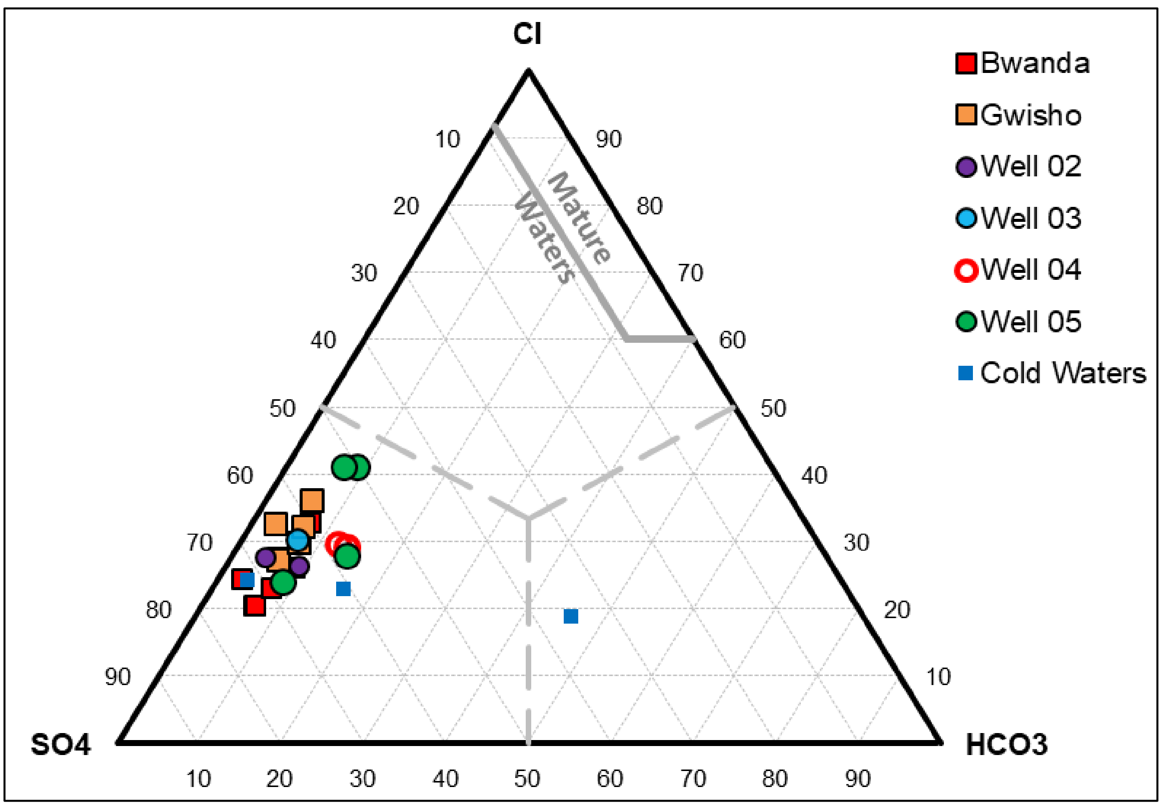

Figure 6. A trilinear diagram relating the relative concentrations of Cl, SO_4, and HCO_3 for water samples for Bwengwa.

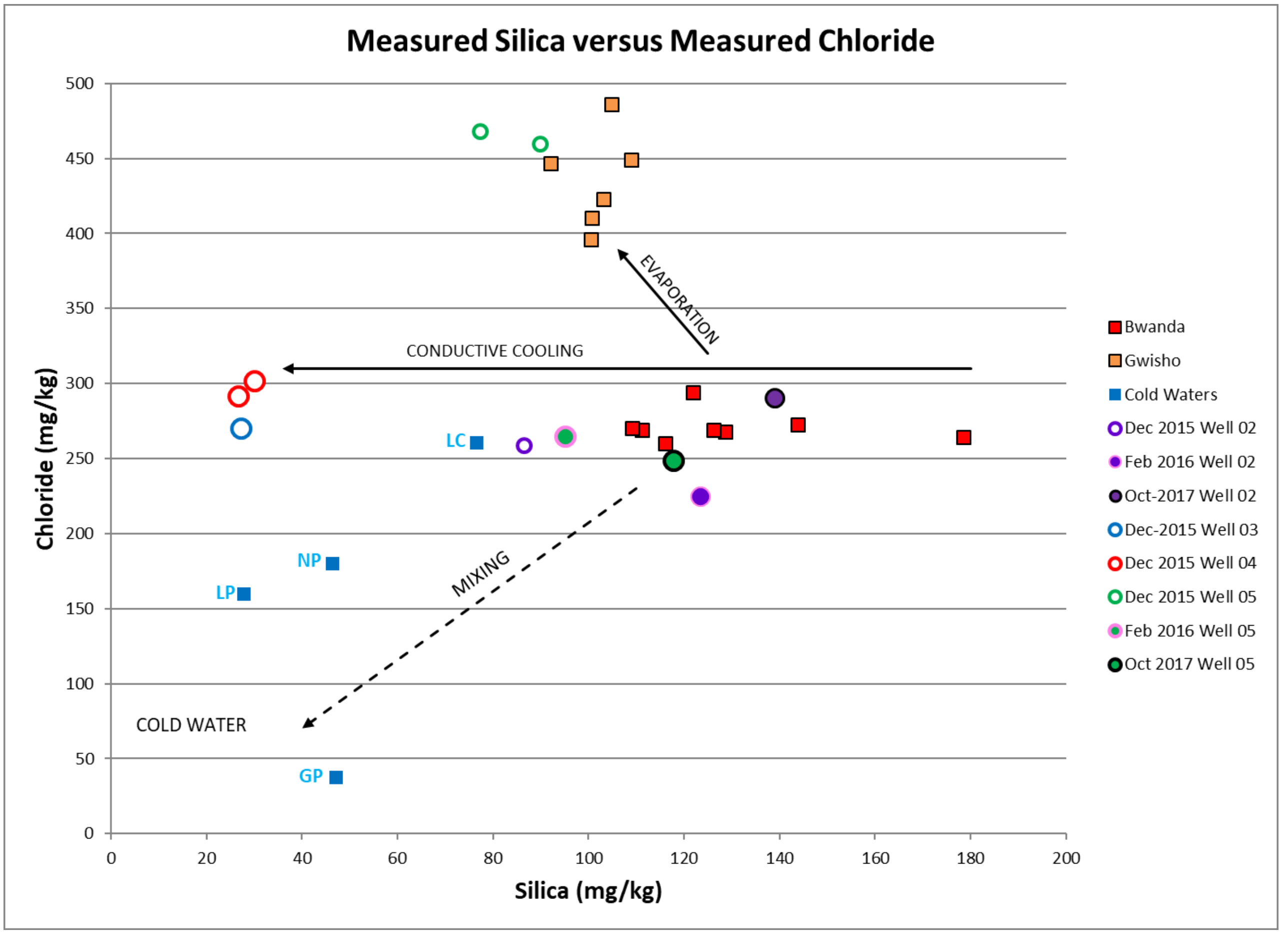

Figure 7. Concentration of chloride and silica from the Bwengwa river area. Possible mechanisms are indicated which may explain the distribution of samples.

Table 1. Typical liquid Geothermometers applied to thermal waters from Bwengwa. Averages for samples collected before 2017. Note that all temperatures are in degrees Celsius.

Site/Well	Quartz (adiabatic)	Na/K	K/Mg	Na/Li
	Fournier (1973)	Fournier (1981)	Giggenbach (1988)	Fouillac and Michard (1983)
Bwanda	143	184	140	164
Bwanda 2017	142	211	152	146
Cold Waters	102	188	79	110
Gwisho	134	164	124	160
Gwisho 2017	140	185	134	133
Well 02	137	193	158	142
Well 02 2017	149	208	178	147
Well 03	80	231	96	145
Well 04	82	113	87	100
Well 05	128	200	133	146
Well 05 2017	141	208	144	149

Geothermometer temperatures calculated from the 2017 samples confirm indications of reservoir temperatures of greater the 140°C from previous samples based on quartz and K-Mg geothermometers (Table 1).

While the commonly used Na/K geothermometers indicate higher (>200°C) temperatures, this often occurs in non-volcanic systems and is often not representative of reservoir temperatures (Figure 7). Relatively high temperature estimates from the Na/K geothermometers suggests these waters are not in equilibrium with the appropriate minerals or that the equilibrium has occurred at some distance from sampling points.

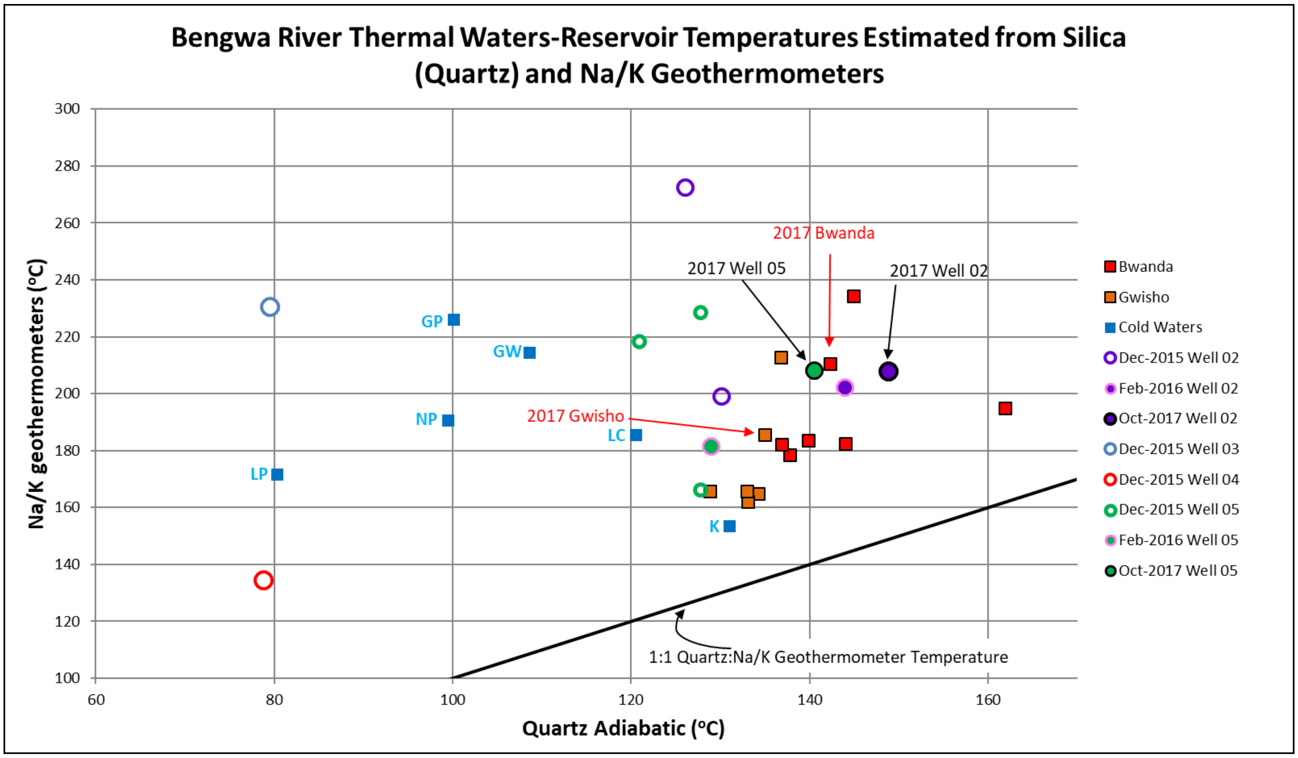

Figure 8. Reservoir temperatures estimated with the quartz adiabatic geothermometer (Fournier 1973) and the Na/K geothermometer (Fournier 1981) are shown.

GEOPHYSICS

Resistivity, gravity, and ground magenetic surveys have been performed at Bwengwa.

Resistivity and gravity

The resistivity survey was an audio-magnetotelluric (AMT) survey with coverage across three areas of hot springs (Figure 9). AMT surveying is not typically as deeply penetrative as MT surveying, meaning the interpretation of the data was truncated at ~1000 m depth (~0 meters above sea level, masl). Even with the relatively shallow depth of penetration, the AMT was able to resolve the unconformity where the impermeable Lower Karoo sediments overlie the Proterozoic (Ptz) metamorphic rocks, as well as the shallow, low-resistivity smectite-rich Upper Karoo sediments that act as a cap to the geothermal reservoir (Figure 10). The AMT appears to show the Upper Karoo cap truncating at or near the Kafue Trough Southern Bounding Fault (SBF) Zone. The geometry of the conglomerates and fault breccias in the Lower Karoo, immediately overlying the Ptz unconformity, are a likely host to lateral outflow of thermal aquifers, and the discontinuities imaged by the AMT could host thermal upflow. The base of the smectite cap shallows to the southeast, before truncating near the wells. Beyond the wells to the southeast is likely uplifted Ptz metamorphic basement.

A gravity survey was conducted in an effort to characterize the structure of the base of the Karoo formations (the likely impermeable cap rock) with respect to the underlying dense Katanga carbonates and Proterozoic metamorphic rocks (the more likely reservoir rock) in the basin northwest of the SBF. A total of 637 stations were collected along 25 survey lines with 1000 m line spacing and 500-1000 m station spacing.

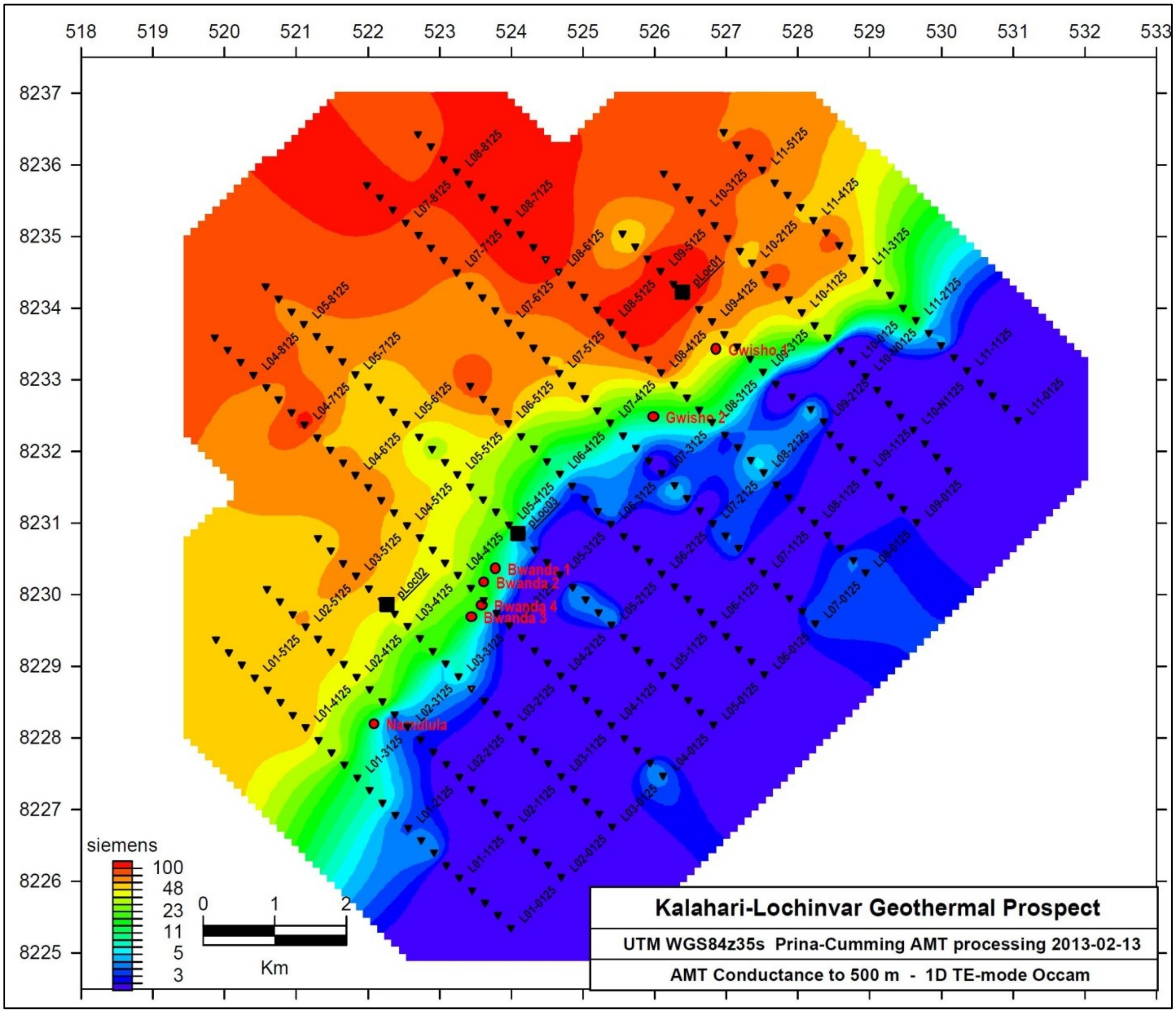

Figure 9. MT conductance to 500 m depth. The yellow-red areas are where clay content is most significant and hydrothermal smectite alteration is particularly intense. Solid triangles show the location of the AMT stations.

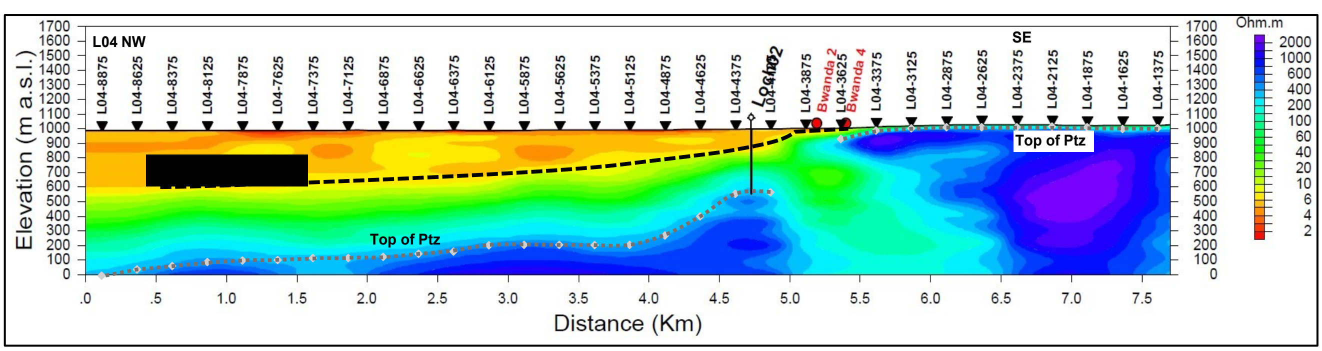

Figure 10. Profile L04 MT resistivity cross-section. Color shading is resistivity from 1D TE-mode smooth inversions.

Magnetic Survey and 3D Modeling

Additional ground magnetic data was collected at Bwengwa to increase the reliability of subsurface imaging of the basement and to allow three-dimensional modeling of the data. The objective of the survey was to evaluate the dip on the primary structure which may be controlling fluid flow. This fault zone is considered to have multiple sub parallel splays. The magnetics identified a range of dips from 34° to 78°. The trend of the fault bends at Sebanzi Hill from ENE northeast of the hill to NE, southwest of the hill. The dips also change from 60-78° northeast of the hill to 34-56° southwest of the hill. These dips were calculated by both BC Consulting (2017) and GEOLOGICA and are indicated on the map in Figure 3. This suggests that the hill is located at the apex of a structural complexity, which may focus the upflow of hot fluids. Furthermore, the magnetics appears to have identified a possible section of carbonate rocks in the basement west of the Gwisho hot springs. Carbonates are typically brittle and break in complex structural settings providing the potential for fracture-hosted permeability. Brittle carbonates are typical reservoir rocks in fault-hosted non-volcanic geothermal systems in the western US and in Turkey.

FLOW TESTS

Loch-02 and Loch-05 were produced during 2017 testing. Prior to flowing each well, a static pressure-temperature (PT) survey was conducted (Figure 11 and Figure 12). During the brief periods of flow, a dynamic PT survey was performed in the flowing well while monitoring pressure in the other well. Geothermal fluid produced from each well was sampled during the flow period.

Both Loch-02 and Loch-05 flow artesian from relatively limited perforated sections of small diameter core hole casing near the bottom of the holes. Loch-02 produced 600-650 kg/hr (through pipe ID=62 mm); and Loch-05 produced 625-725 kg/hr increasing throughout the test (through 46 mm ID tubing). PT surveys confirmed that that fluids produced from Loch-02 and Loch-05 are ≥100°C at the top of the basement formation.

Results of this preliminary core hole testing indicate that the geothermal fluids discharge along the SBF/Karoo interface over a subsurface extent of at least 1.2 km extending from Loch-05 to the Bwanda hot springs, roughly perpendicular to strike from the SBF.

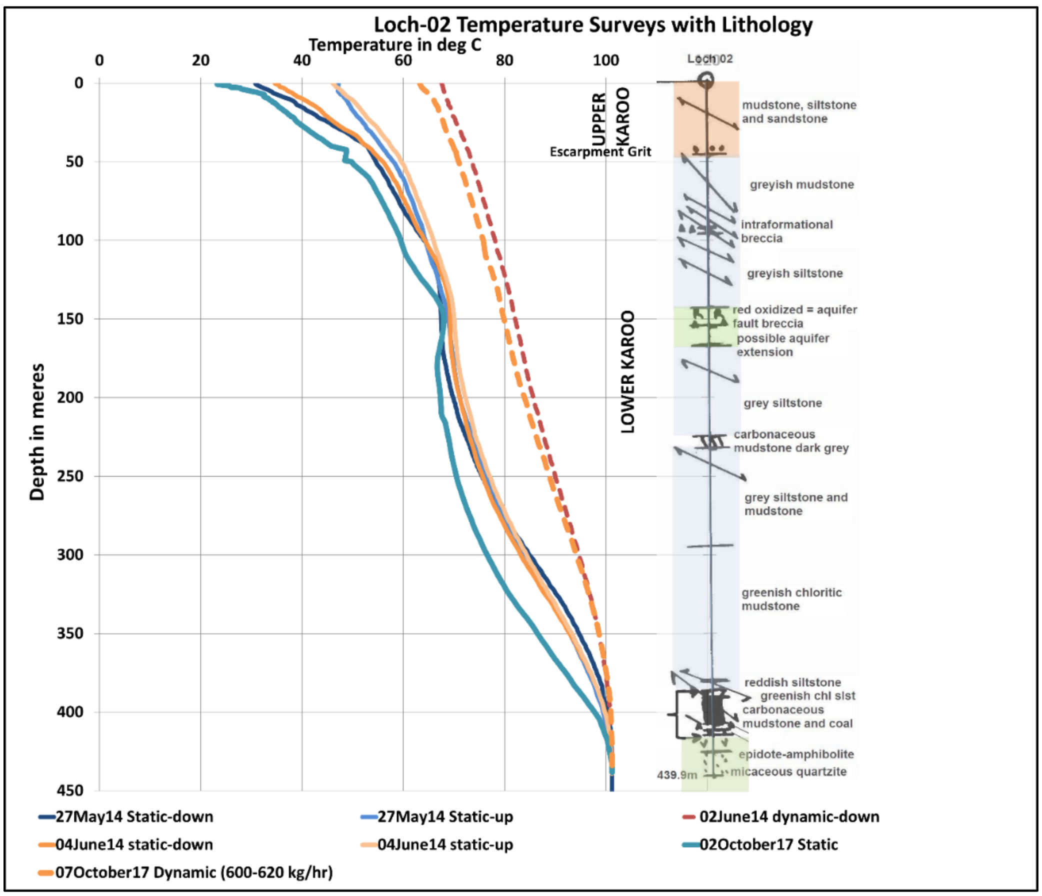

Figure 11. Well Summary plot of Loch-02.

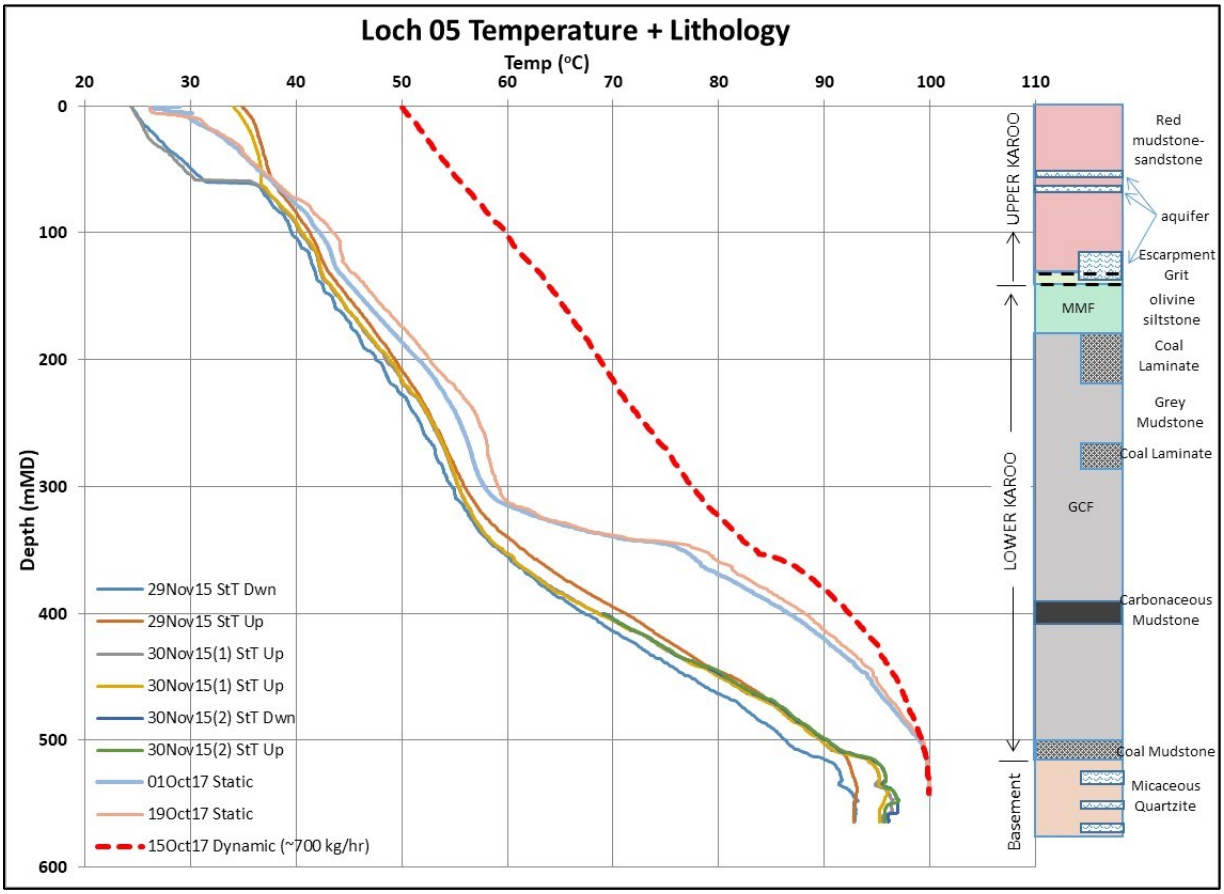

Figure 12. Well Summary plot of Loch-05.

UPDATED CONCEPTUAL MODEL

The conceptual model of the Bwengwa River Geothermal System is that of a fault-based non-volcanic geothermal system composed of deeply circulating water heated by natural conductive heat flow. In well known fault-based geothermal systems, locally derived meteoric water circulates along permeable faults and fractures related to extensional tectonic settings to depths where temperatures are elevated and water is heated by the rock; the bouancy of hot water causes it to rise along other permeable faults. The extensional stress supports permeability at fault and fracture intersections and complexities (Faulds et al., 2012; Faulds et al., 2016).

At Bwengwa River, cold local meteoric water circulates to depths of 3-5 km along permeable faults and fractures created by structural complexities developed by the intersection of NW-SE extensional stresses and the SBF. These extensional stresses have transformed and reactivated the ENE to NE trending transform SBF, an ancient plane of weakness, into a complex fault zone with oblique movement. Complexities are indicated by a well-mapped bend at Sebanzi Hill between Gwisho and Bwanda hot springs, and SE-NW cross faults. High flow-rate, near-boiling springs reflect upflow of hot water along this structure. The hot springs and the fluid in the wells originate from the same source as evidenced by very similar temperature, chemistry and geothermometry.

The WSW-ENE trending SBF is developed at the NW end of a NW-SE trending Basement uplift (possibly a horst) which is flanked by prominent embayments to the ENE (e.g. the Mazabuka synclinorium) and to the WSW (e.g. the Monze embayment). Displacement along the SBF is NW-SE to WNW-ESE normal dip-slip with a limited component of right lateral (dextral) oblique slip. This geometry is supported by the complete lack of shear fabrics within the SBF (Harrison, 2018).

The cross section through the SBF in Figure 13 illustrates the updated conceptual model. An upflow at ~150°C ascends bouyantly along splays and transtensionally-propped open fractures in the Southern Bounding Foult Zone (SBFZ) beneath the Karoo basin sediments, and outflows both basinward and updip within the the damage zone in the basement rocks along the SBF to expressions at Bwanda and the Gwisho Hot Springs. Where the basement rocks include carbonates, brittle fracturing and/or karstification along paleo-faults enhances permeability. Recharge of meteoric water occurs along subsidiary faults conjugate to the SBF, as well as at the structural complication and elevated topography of Sebanzi Hill.

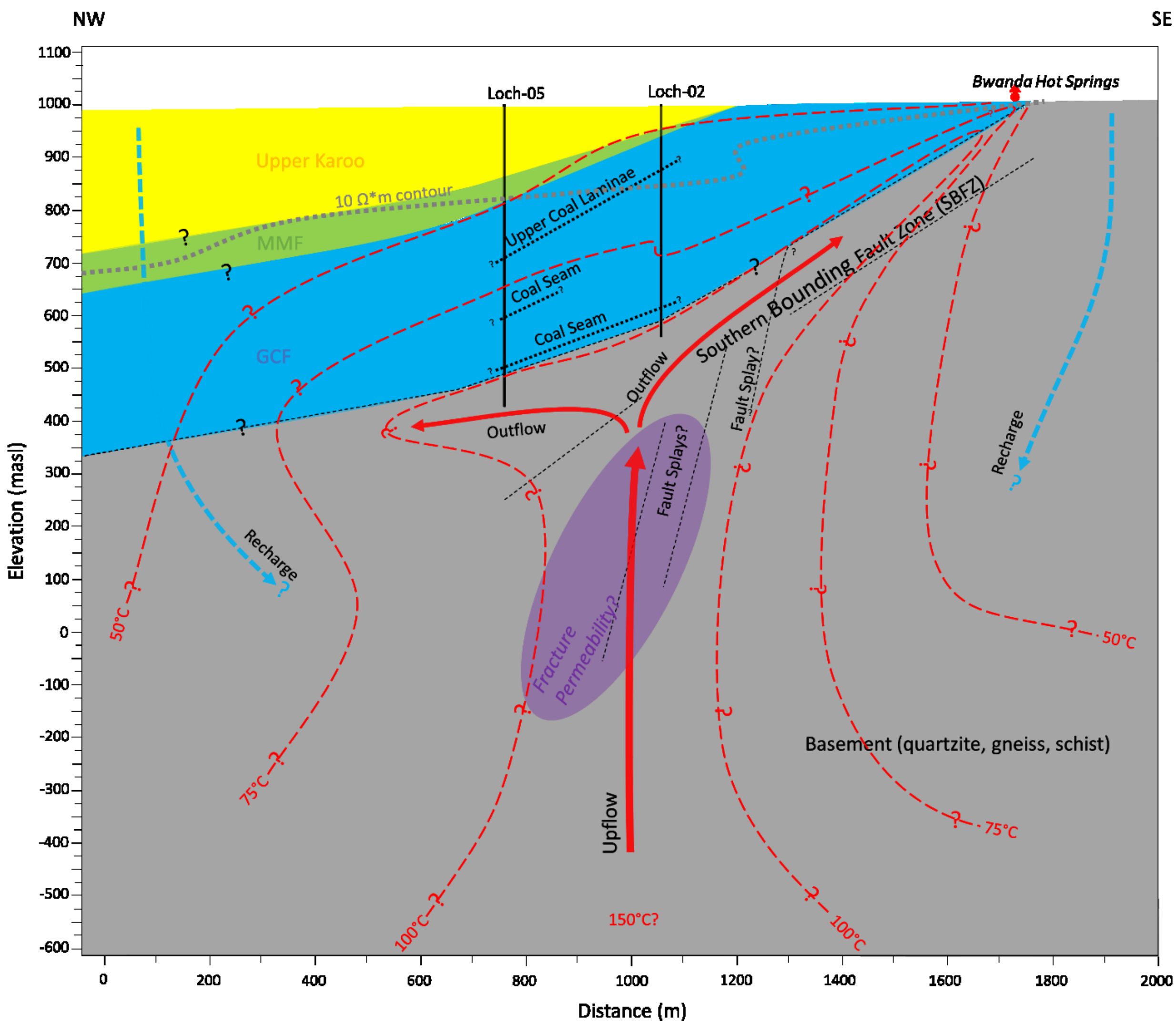

Figure 13. Conceptual cross section NW-SE through the Southern Bounding Fault Zone.

UPDATED POWER DENSITY RESERVOIR CAPACITY ESTIMATE

Heat-in-place estimates for geothermal systems are common but often overestimate resource capacity by large factors, even orders of magnitude, due to unreasonably optimistic recovery factors (Grant, 2015). Power density estimates can often be as accurate as more complex heat-in-place estimates at the exploration stage as they rely on fewer assumptions and are calibrated against a large number of known operating fields (Wilmarth and Stimac, 2015).

A power density estimate was made for the Bwengwa reservoir. The estimate was made using the model provided by Cumming (2016) which assumes log-normal distributions. Areas were based on the drilled wells and hot springs. The P90 area is a 500 m buffer around wells Loch-02 and Loch-05. This area does not include wells Loch-03 and Loch-06, which were completed in an intermediate aquifer and for which no samples were collected. This area is ~1.1 km^2. The P10 (optimistic) area is a 750 m buffer of a line basin-ward and parallel to the SBF between the three areas of hot springs. This area is ~13.3 km^2.

A range of power densities was chosen based on the plot of Power Density vs Average Reservoir Temperature for 80 operating fields (Figure 14). The Bwanda and Gwisho Hot Springs have average cation geothermometers of up to ~150°C. Therefore, an estimated temperature range of 125-175°C was used (minimum reservoir temperature of 125°C, average reserves reservoir temperature of 150°C). The high hot spring flow and apparent high permeability encountered in the temperature gradient wells justifies using a larger power density range than indicated by the main trend line in the plot ("The Main Sequence") and would be analogous to other shallow high-permeability reservoirs in the U.S. Basin and Range. This corresponds to an expected power density range of 1-15 MW/km^2 (Figure 14).

This model handicaps undiscovered resources with exploration confidence factors for the probability of discovering commercial temperature, permeability and benevolent reservoir chemistry. Given the measured temperatures of >100°C, a $P_{Temperature}$ was chosen of 90%. A lower $P_{Permeability}$ of 70% was chosen, typical of other undiscovered resources at this stage of exploration in similar favorable structural settings. Reservoir chemistry is rarely a determinant of project success in the Basin and Range and consequently a $P_{Chemistry}$ of

99% was chosen. The combination of these factors results in a Probability of exploration success (POS_{expl}, the chance that at least one commercial well will exist) of 62% (Figure 15).

The probabilistic power density estimate discounted by the POS_{expl} yields an expected mean capacity of 25 MWe with a P50 (most likely) capacity of 9 MWe. A discovered 150°C resource has an expected power capacity of 2-93 MWe (P90-P10) with a most likely value of 15 MWe (P50) as shown in Figure 15 and Figure 16.

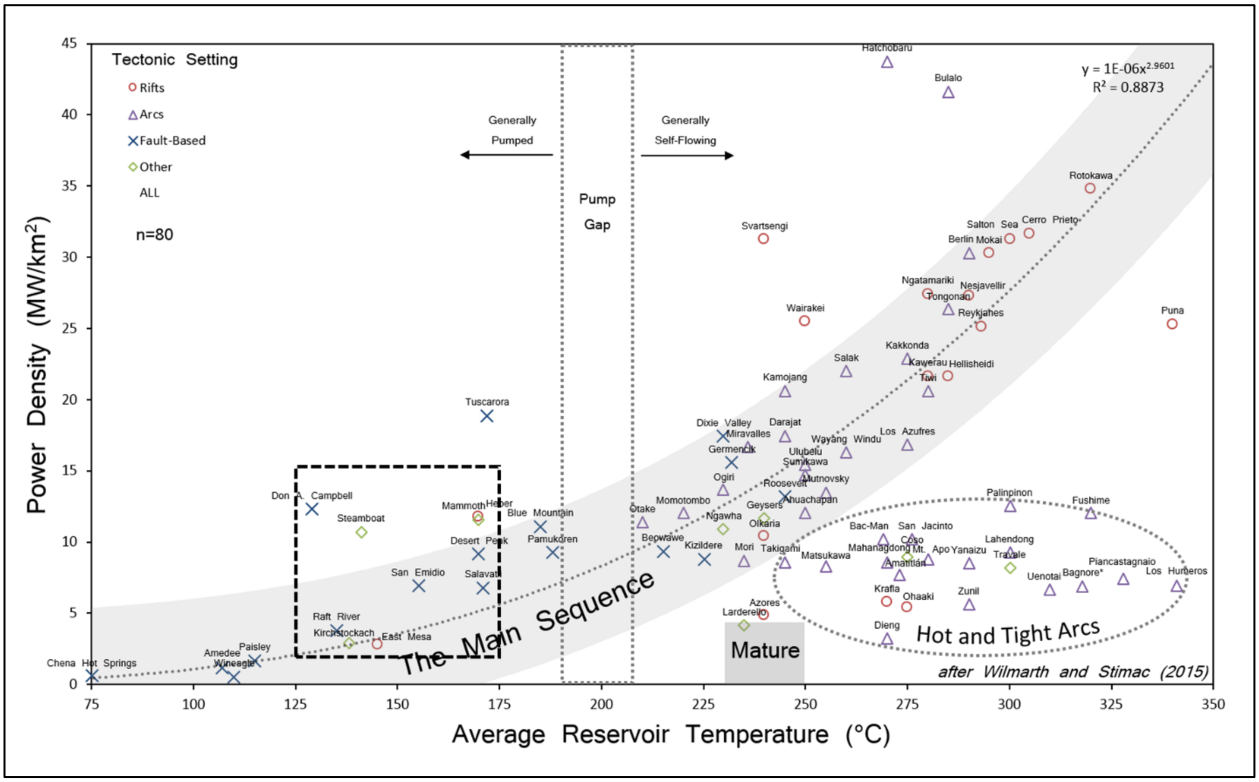

Figure 14. Power Density vs Average Reservoir Temperature for 80 operating fields, after Wilmarth and Stimac (2015). Estimated range of reservoir temperature and power density for Bwengwa indicated with black dashed rectangle.

Geothermal Power Capacity Reserve Estimation: based on Lognormal Distributions of Area and Power Density

This spreadsheet is used to constrain geothermal resource capacity assessments based on analogies to the area and power density of developed fields.
In this spreadsheet, 90% of all cases are larger than P90 and 10% are larger than P10. That is, P90 is the smaller number and P10 is larger.

EXLORATION: Is it there?

Assuming a likely exploration geoscience program and drilling program, what is the percent confidence that at least one well is commercial

	Confidence in temperature.		Confidence in permeability. Commercial mDarcy		Confidence in chemistry. Not corrosive or scaling		Probability of exploration success
	PTemperature		PPermeability		Pchemistry		POSexpl
Exploration Confidence	0.90	*	0.70	*	0.99	=	0.62

APPRAISAL AND DEVELOPMENT: Assuming it's there, how big is it?

Cumulative confidence of representative optimistic case = **10%** That is, the larger, more optimistic case is assumed to be P10

Temperature range of permeable reservoir area from resource conceptual model. This should be consistent with assumed power density distribution.

Startup average production temperature for P90 reserves = **150** °C **125** °C = minimum temperature for P10 reservoir

Nu and Sigma are the mean and variance in log units required for specifying lognormal distributions in tools like @RISK

Representative Cases				Pessimistic	Middle	Optimistic					
		P99	P90	P90	P50	P10	P10	P01	Mean	nu	sigma
Area > 125°C	**(km^2)**	0.4	1.1	**1.1**	3.8	**13.3**	13.3	36.7	6.1	1.34154	0.97244
Power Density 125 to 150 °C	**(MWe/km^2)**	0	12	**1**	4	**15**	15	45	7	1.35403	1.05655
MWe Capacity		1	2	2	15	93	93	418	42	2.69556	1.43594

EXPECTED POWER CAPACITY RESERVES (based on analogous reservoirs used to assess confidence in power density and area)

Expected Mean Capacity = 25 MWe = [Probability of Exploration Success] * [Mean Capacity of Development Assuming Exploration Success]

Expected P50 Capacity= 9 MWe = [Probability of Exploration Success] * [P50 Capacity of Development Assuming Exploration Success]

Figure 15. Bwengwa Reservoir Potential Power Capacity reserve calculation based on lognormal distributions of Area and Power Density. After Cumming (2016).

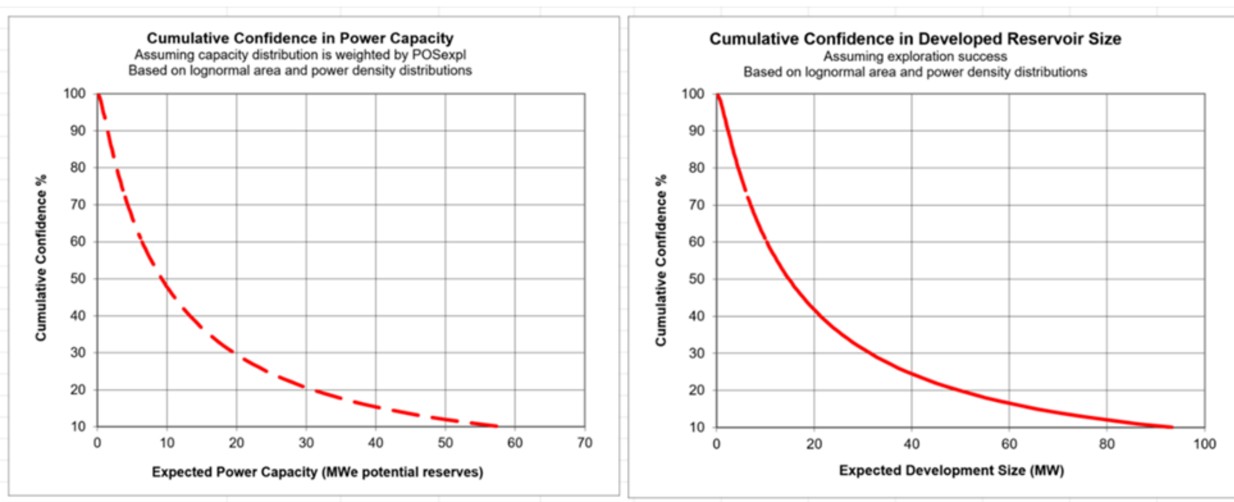

Figure 16. Cumulative Confidence in Power Capacity (left), and Cumulative Confidence in Developed Reservoir Size (right) after Cumming (2016).

NEXT STEPS: DRILLING

During the next drilling campaign, KGE intends to drill through the upper basement rocks and penetrate the top of the geothermal reservoir at a depth of 1000-1500 m. Work performed in 2017 confirmed that the deeper and hotter ~150°F) geothermal system believed to underlie the area and provide the source of thermal water discharged in the springs and Loch-02 and Loch-05 wells is within the basement rocks where permeability is fracture controlled. Targeting of specific well locations is in progress. The final targets will be based on a detailed examination of faulting and fracturing and the most likely structural settings for permeable fractures such as extensional/transtensional fault intersections (i.e. the NE trending SBFZ and subparallel splays) and in the karsted (dissolved) limestone immediately surrounding faults in marble basement rocks. Likely locations include the deeper projected intersection of the complexities of the SBF and the upper basement forming reservoir north and south of Loch-02, and the off-set and down-dropped marble basement rocks adjacent to the SBF suggested by geophysics and SBF mapped splays north of Sebanzi Hill.

REFERENCES

BC Consulting; (2017); *Notes on 3D modelling of magnetic data acquired over the Bwenga River Project Zambia*; Internal report dated July 21, 2017.

Bufford, K.M., Atekwana, E.A., Abdelsalam, M.G., Shemang, E., Atekwana, E.A, Mickus, K., Moidaki, M., Modisi, M.P. & Molwalefhe, L., 2012. *Geometry and faults tectonic activity of the Okavango Rift Zone, Botswana: Evidence from magnetotelluric and electrical resistivity tomography imaging*. Journal of African Earth Sciences, Vol. 65, pp 61-71. April 2012.

Coolbaugh, M.F., Sladek, C., Kratt, C., Shevenell, L., and Faulds, J.E.; (2006); *Surface Indicators of Geothermal Activity at Salt Wells, Nevada, USA, Including Warm Ground, Borate Deposits, and Siliceous Alteration*; GRC Transactions, Vol. 30.

DiPippo, R., and Kitz, K.; (2015); *Geothermal Binary Power Plants at Raft River, San Emidio, and Neal Hot Springs: Part 1—Plant Descriptions and Design Performance Comparison*; GRC Transactions, Vol. 39.

Drakos, P., Spielman, P., Björnsson, G.; (2011); *Jersey Valley Exploration and Development*; GRC Transactions, Vol. 35.

Faulds, James E.; Hinz, Nicholas; Kreemer, Corne; (2012); *Structural and Tectonic Controls of Geothermal Activity in the Great Basin Region, Western USA;* Proceedings of the New Zealand Geothermal Workshop, Vol. 34.

Faulds, J.; Hinz, N.; Coolbaugh, M.; Depolo, C.; Siler, D.; Shevenell, L.; Hammond, W.; Kreemer, C.; Queen, J.; (2016); *Discovering Geothermal Systems in the Great Basin Region: an Integrated Geologic, Geochemical, and Geophysical Approach for Establishing Geothermal Play Fairways;* Proceedings: Workshop on Geothermal Reservoir Engineering, Vol. 41.

GEOLOGICA; (2013); *Preliminary Geothermal Resource Assessment: Bwengwa River Geothermal Area, Zambia*; Internal report dated February 2013.

GEOLOGICA; (2016); *Update: Preliminary Resource Assessment, Bwengwa River Geothermal Project*, Internal report dated April 2016.

Grant, M.A., and Bixley, P.F.; (2011); *Geothermal Reservoir Engineering*; Academic Press.

Harrison, P., 2012. The stratigraphy and regional tectonic setting of the Karoo sediments on the southeastern margin of the Kafue trough, Zambia. Unpublished report prepared for Kalahari GeoEnergy. Prepared by Peter Harrison, 16 pp.

Harrison, P.; *Some comments on the sense of movement and direction of maximum extension along the SBF*. Internal memo date January 22, 2018.

Legg, C.A., 1974. A reconnaissance survey of the hot and mineralized springs of Zambia. Republic of Zambia Ministry of Mines and Industry, Economic Report of the Geological Survey No. 50.

Hinz, N.H., Faulds, J.E., and Coolbaugh, M.F. (2014); *Association of Fault Terminations With Fluid Flow in the Salt Wells Geothermal Field, Nevada, USA*; GRC Transactions, Vol. 38.

Rhodes, G.T., Faulds, J.E., and Teplow, W.; (2010), *Structural Controls of the San Emidio Desert Geothermal Field, Northwestern Nevada*; GRC Transactions, Vol. 34.

Wilmarth, M., and Stimac, J. (2015). *Power Density in Geothermal Fields*. Proceedings, World Geothermal Congress, Melbourne, Australia.